J Membrane Biol (2010) 234:183–194
DOI 10.1007/s00232-010-9245-6

Membrane Organization and Regulation of Cellular Cholesterol Homeostasis

María S. Jaureguiberry · M. Alejandra Tricerri · Susana A. Sanchez · Horacio A. Garda · Gabriela S. Finarelli · Marina C. Gonzalez · Omar J. Rimoldi

Received: 30 October 2009 / Accepted: 4 March 2010 / Published online: 25 March 2010

Abstract An excess of intracellular free cholesterol (Chol) is cytotoxic, and its homeostasis is crucial for cell viability. Apolipoprotein A-I (apoA-I) is a highly efficient Chol acceptor because it activates complex cellular pathways that tend to mobilize and export Chol from cellular depots. We hypothesize that membrane composition and/or organization is strongly involved in Chol homeostasis. To test this hypothesis, we constructed a cell line overexpressing stearoyl coenzyme A (CoA) desaturase (SCD cells), which modifies plasma membrane (PM) composition by the enrichment of monounsaturated fatty acids, and determined this effect on membrane properties, cell viability, and Chol homeostasis. PM in SCD cells has a higher ratio of phospholipids to sphingomyelin and is slightly enriched in Chol. These cells showed an increase in the ratio of cholesteryl esters to free Chol; they were more resistant to Chol toxicity, and they exported more caveolin than control cells. The data suggest that cell functionality is preserved by regulating membrane fluidity and Chol exportation and storage.

Keywords Stearoyl CoA desaturase · Human apolipoprotein A-I · Membrane heterogeneity · Cholesterol transport · Chinese hamster ovary cells · Intracellular cholesterol storage · Caveolin · Cytotoxicity

M. S. Jaureguiberry · M. A. Tricerri · H. A. Garda · G. S. Finarelli · M. C. Gonzalez · O. J. Rimoldi (✉)
Instituto de Investigaciones Bioquímicas de La Plata (INIBIOLP), CONICET/UNLP, Facultad de Ciencias Médicas, Calles 60 y 120, La Plata 1900, Buenos Aires, Argentina
e-mail: ojrimoldi@hotmail.com

S. A. Sanchez
Laboratory for Fluorescence Dynamics, University of California-Irvine, Irvine, CA, USA

Cholesterol (Chol) plays several structural and metabolic roles that are crucial to human biology. In particular, in membranes, it regulates fluidity and different cell signaling events by partitioning into domains of selective composition as caveolae and other sphingolipid-rich domains (Jacobson et al. 2007). Cellular Chol can be synthesized de novo or incorporated via the uptake of Chol-containing lipoprotein particles. On the other hand, extrahepatic cells lack metabolic pathways for Chol catabolism, and thus the excess must be either exported or recruited into nontoxic cellular compartments. Although the mechanisms seem to be opposite, both depend on cellular type and on intracellular trafficking, which is regulated by several signaling pathways (Prinz 2007). Chol is transported from the endoplasmic reticulum to the plasma membrane (PM) by protein-mediated and vesicular pathways. The signaling events involved are complex and not completely understood. Sterol carrier protein 2 (SCP-2) has been related with different lipid transports, such as phosphatidylinositol, sphingomyelin (SM), and phospholipids. It has been involved in intracellular traffic of Chol to the PM and recent data show that SCP-2 interacts with caveolin-1, both within cytoplasm and at the PM (Schroeder et al. 2001, 2007). Thus, a close interaction between these proteins seems to modify intracellular distribution of signaling lipids to PM lipid rafts/caveolae.

The apolipoprotein-mediated cellular Chol release requires a specific interaction of apolipoproteins with proteins on the cell surface. There is a large body of evidence that the adenosine triphosphate (ATP) binding cassette A1 (ABCA1) catalyzes the concurrent loading of apolipoproteins with phospholipids and Chol (Smith et al. 2004), but there are also different pieces of evidence indicating that these events occur separately in time and in different specialized domains of the cell membrane

(Fielding et al. 2000; Yancey et al. 2003). It was proposed that ABCA1 promotes flipping of lipids from the inner to the outer membrane leaflet by a process driven by its ATPase activity (Oram 2002). Interestingly, there is some controversy on the role of lipid rafts in Chol efflux. Although Mendez et al. (2001) suggest that apolipoprotein A-I (apoA-I) preferentially acquires Chol from loosely packed microdomains, Storey et al. (2007) demonstrated that apoA-I removes Chol with higher efficiency from the lipid raft. The molecular mechanisms of intracellular Chol pool mobilization toward the cell membrane mediated by apoA-I are also poorly understood. ABCA1 seems to favor the removal of Chol meant to be the substrate for the esterifying enzyme acyl coenzyme A (CoA):Chol acyltransferase (Oram and Heinecke 2005) that would otherwise accumulate as cytosolic cholesteryl ester in lipid droplets. It was proposed that apoA-I induces the transport of intracellular Chol to cell-surface caveolae, possibly in part through the stimulation of caveolin expression (Sviridov et al. 2001).

There is strong evidence that lipid arrangement in biological membranes is heterogeneous. Small changes in physicochemical variables such as Chol content, variations of lipid head group chemistry, or protein interactions might induce growth or coalescence of certain types of lipid domains, which could in turn modulate membrane-associated physiological signaling. To characterize the importance of membrane composition and lateral organization on Chol homeostasis, we constructed a stable cell line with a permanent modification in the PM lipids and further analyzed the influence of this composition on the Chol homeostasis and cell viability. The overexpression of stearoyl CoA desaturase (SCD cells) alters the phospholipid fatty acid composition without changing the expression levels of ABCA1 (Sun et al. 2003).

Experimental Procedures

Materials

ApoA-I from healthy human serum (donated by Banco de Sangre, Instituto de Hemoterapia de la Provincia de Buenos Aires, La Plata, Argentina) was isolated and purified as previously described (Tricerri et al. 1998). Purity was higher than 95% as estimated by sodium dodecyl sulfate (SDS)–polyacrylamide gel electrophoresis (PAGE) with Coomassie blue staining. Laurdan (6-lauroyl-2-(dimethylamino) naphthalene) was purchased from Molecular Probes (Eugene, OR). Tris (hydroxymethyl) aminomethane hydrochloride (Trizma HCl), 3-[4,5-dimethylthiazol-2-yl]-2, 5-diphenyl tetrazolium bromide (MTT), methyl-β-cyclodextrin (MβCD), Oil Red O and lipids used as standards for thin-layer chromatography (TLC); egg phosphatidylcholine, free and esterified Chol, brain SM, phosphatidylinositol, phosphatidylserine, and phosphatidyl ethanol amine were obtained from Sigma-Aldrich Biochemicals (St. Louis, MO); minimal essential medium (MEM) and the antibiotic–antimycotic mixture were obtained from Invitrogen (Carlsbad, CA). Fetal bovine serum (FBS) was purchased from Bioser (Buenos Aires, Argentina), and [^{3}H] Chol was obtained from Amersham Biosciences (Pittsburgh, PA).

Polyclonal anti-apoA-I antibody was obtained by injecting purified human apoA-I in rabbits and further purifying the IgG fraction from plasma by Hi-trap columns (Pharmacia, Piscataway, NJ). A polyclonal anti-rat SCD-1 antibody was obtained by cloning the fragment corresponding to the 85 N-terminal amino acid section of the cDNA into the plasmid pGEX-4T-1 (Amersham Biosciences, Pittsburgh, PA). The pGEX-SCD-1 construct was expressed in *Escherichia coli* BL21 cells, and the glutathione-S-transferase fusion protein was purified according to the manufacturer's instructions. The purified bacterial expressed fusion protein was used as an immunogen on rabbit. Antibodies against ABCA1 and caveolin-1 proteins were purchased from Santa Cruz Biotech (Santa Cruz, CA).

Methods

Construction of Stable Cell Lines Overexpressing Stearoyl CoA Desaturase (SCD Cells)

We created a stable cell line overexpressing the enzyme stearoyl-CoA-desaturase (SCD-1) according to Sun et al. (2003). The full-length SCD-1 cDNA was subcloned in the plasmid pcDNA3.1-Hygro to generate pcDNA3.1-SCD-1, and the stable transfection was performed with Lipofect-AMINE 2000 (Invitrogen). A clone resistant to hygromycin was selected, expanded, and frozen in liquid N_2 for further experiments. Cells transfected with the plasmid without the SCD-1 insert were considered as control cells for all experiments.

The SCD-1–mRNA overexpression in the selected clone was assessed by Northern blot analysis. Total cell RNA was isolated with a Wizard RNA isolation system (Promega, Madison, WI) according to the manufacturer's instructions. Twenty micrograms of total RNA were size fractionated on a 1% agarose/formaldehyde gel and then transferred to a Zeta-Probe nylon membrane (Bio-Rad, Richmond, CA). SCD- and β-actin probes were prepared by incorporating [^{32}P] deoxycytidine 5′-triphosphate by random prime labeling. Northern blot hybridization analyses were performed as described by Sambrook et al. (1989). The radioactive signals for mRNAs of SCD-1 were quantified with a PhosphorImager apparatus (Molecular Dynamics, Sunnyvale, CA). Signal was normalized to

mRNA for β-actin with the desaturase mRNA probed on the same gel.

Next, we verified the protein level in our stable cell line by Western blot analysis. Total cell protein samples (150 μg per lane) were analyzed by SDS–PAGE and blotted onto a Hybond-enhanced chemiluminescence (ECL) nitrocellulose membrane (Amersham Biosciences, Little Chalfont, England, UK). The membrane was probed with the anti-SCD-1 antibody (1:1000 dilution) and then with horseradish peroxidase-conjugated anti-rabbit (Sigma-Aldrich) (1:3000 dilution) by phosphate-buffered saline (PBS; pH 7.5) containing 3% nonfat dried milk for saturation and incubation with antibodies. Washes were carried out with PBS as well. Peroxidase activity was revealed with Pierce ECL Western blotting substrate (Pierce, Rockford, IL).

In addition, we analyzed membrane fatty acid composition. Briefly, cellular fractions corresponding to PM were isolated (see below), lipids extracted according to Folch et al. (1957), and samples esterified with F_3B at 64°C for 3 h. Fatty acid composition of cell total lipids was determined by gas–liquid chromatography of their methyl esters. Samples were injected into an Omega Wax 250 (Supelco, Bellefonte, PA) capillary column of 30 m, 0.25 mm inner diameter, and 0.25 μm film. The temperature was programmed to obtain a linear increase of 3°C/min from 175 to 230°C. The chromatogram peaks were identified by comparison of their retention times with those of authentic standards (Grain Fatty Acid Methyl Ester Mix; Supelco, Bellefonte, PA).

Finally, we checked by Western blot testing the ABCA1 protein expression in our cell line compared to control cells to discard alterations in its level due to desaturase overexpression.

Cell Culture

Cells were cultured as described by Gonzalez et al. (2008). Chinese hamster ovary (CHO) cells were seeded in 10-cm-diameter plates and incubated until confluence in MEM supplemented with penicillin/streptomycin solution (100 units/ml) and 10% FBS at 37°C in a 5% CO_2 atmosphere.

Evaluation of Cellular-free and Esterified Chol

Control and SCD cells were grown until confluence. Next, cell monolayers were washed with PBS and incubated overnight with serum-free medium containing 0.5 μCi/ml [^{3}H] Chol and 2 mg/ml bovine serum albumin. After 24 h equilibration with MEM containing 1 mg/ml of bovine serum albumin, monolayers were washed twice with PBS and treated for 12 h with serum-free medium, containing or not containing 12 μg/ml of apoA-I. Media were collected and cells scraped for lipid extraction by the method of Bligh and Dyer (1959). Sterol species were separated by high-performance TLC on a silica gel plate with concentrating zone (Whatman, Schleier-Schuell, England, UK) and developed in hexane/ethyl ether/acetic acid (80:20:1 by volume). Lipid spots corresponding to cholesteryl esters (CE) and unesterified Chol (FC) were identified by staining with I_2 vapor and comigration with authentic standards. Appropriate spots were scraped and quantified by scintillation counting.

Membrane Isolation and Lipid Characterization

We followed the technique of Mander et al. (1994), with modifications. Cell monolayers were grown to confluence, washed three times with PBS, scraped, and resuspended in 900 μl buffer 10 mM HEPES (N-[2-hydroxyethyl] piperazine-N′[2-ethanesulfonic acid]), 0.25 M Sacarose, 1 mM EDTA (ethylenediaminetetraacetic acid) pH 7.4 to get approximately 1.5–2 $\times$ 10^7 cells/ml. Cells were lysed in a glass to glass homogenizer with $\sim$20 strokes and centrifuged at 16,000*g* for 15 min. A gradient of Nicodenz–Ficoll was handmade by the step-by-step addition of 45% Nicodenz solution followed by Ficoll gradient between 1 and 22%. The supernatant of the cell sample was loaded on top of the test tube and ultracentrifuged in a L8.70 M Ultracentrifuge at 238,000*g* in a SW 60 Ti Rotor (Beckman Coulter, Fullerton, CA) for 16 h at 4°C. Two-hundred-microliter fractions were collected from the top of the gradient tube, protein content in each fraction was measured (Bradford 1976), and fractions corresponding to PM were pooled and characterized by means of standard enzyme markers and electron microscopy. Lipids were extracted according to the procedure of Bligh and Dyer (1959) and separated by TLC on silica gel G 60 plates with concentrating zone (Merck, Darmstadt, Germany). We used two successive development systems for polar lipids chloroform/methanol/ammonium/water (70:25:3.5:1.5, by volume) and chloroform/methanol/acetic acid/water (80:10:2:0.76, by volume), followed by a mixture to better develop neutral lipids petroleum ether/ethyl ether/acetic acid (80:20:1, by volume). Then the plate was spread with ethanol–sulfuric acid (5%) and heated until complete calcination. Spots corresponding to each lipid were identified with appropriate standards and quantified by Image Quant software (Amersham Biosciences, Piscataway, CA).

Cell Viability

Control and SCD cells (with or without the addition of 20 μg/ml apoA-I) were incubated as described above, and the MTT reduction assay was carried out as previously described (De Felice et al. 2001). Briefly, cells were

incubated with 0.5 mg/ml MTT at 37°C for 4 h to allow MTT reduction to formazan blue by metabolically active cells. One hundred microliters of 0.01 N HCl containing 10% SDS was added and kept overnight to each well to lyse cells and solubilize formazan crystals. Optical density was measured at 570 nm in a DTX 880 Multimode Detector (Beckman Coulter, Fullerton, CA). In a separate experiment, media were collected, and the release of the cytoplasmic enzyme lactate dehydrogenase (LDH) was measured by decrease of optical density at 340 nm (commercial kit, Wiener Lab, Rosario, Argentina).

Oil Red O Lipid Droplets Staining

Intracellular neutral lipids were stained with Oil Red O. Briefly, cell monolayers were rinsed with PBS and fixed for 1 h with PBS plus 10% formaldehyde. Next, staining was performed by covering with 0.5% Oil Red O in isopropanol for 2 h, followed by extensive washing. Representative photomicrographs are shown for control and SCD cells.

Laurdan Generalized Polarization (GP) Imaging and Quantification

Laurdan is used as a membrane probe because of its large excited-state dipole moment, which results in its ability to report the extent of water penetration into the bilayer surface as a result of the dipolar relaxation effect (Weber and Farris 1979). Water penetration has been correlated with lipid packing and membrane fluidity (Parasassi et al. 1997). If Laurdan is solubilized in a lipid structure (i.e., a membrane), its spectrum will sense the environment and shift according to the water content of the bilayer. The quantification of the spectral shift is given by

$$\mathrm{GP} = \mathrm{I440} - \mathrm{I490}/\mathrm{I440} + \mathrm{I490}, \quad (1)$$

where I440 and I490 are the emission intensities at 440 and 490 nm, respectively. A full discussion of the use and mathematical significance of GP can be found elsewhere (Bagatolli et al. 2003; Parasassi and Gratton 1995; Sanchez et al. 2007a, b). Images were collected on a scanning two-photon fluorescence microscope designed at the Laboratory for Fluorescence Dynamics (University of California, Irvine, CA) as described previously (Sanchez et al. 2007a; So et al. 1995). A mode-locked titanium sapphire laser (Mira 900; Coherent, Palo Alto, CA) pumped by a frequency-doubled Nd:vanadate laser (Verdi; Coherent) set to 780 nm was used as the two-photon excitation light source. The microscope setup was fixed as described previously. A two-channel detection system was attached for GP image collection (Sanchez et al. 2007a). The fluorescence was split in two channels with a Chroma Technology 470DCXR-BS dichroic beam splitter in the emission path. Interference filters (Ealing 490 and Ealing 440) were placed in the emission paths to further isolate the two desired regions of the emission spectrum (440 ± 10 nm and 490 ± 10 nm), which were collected simultaneously by separate detectors. Two simultaneous 256 × 256–pixel images (centered at 490 nm emission, and centered at 440 nm emission) were obtained from the cells, which were processed applying the GP formula (Eq. 1) to each pixel by the SimFCS program (Laboratory for Fluorescence Dynamics). Corrections for the wavelength dependence of the emission detection system were accomplished through the comparison of the GP value of a known solution (Laurdan in dimethyl sulfoxide) (Sanchez et al. 2002) taken on an ISS Inc. model PC1 steady-state fluorometer and then in the microscope.

SCD or control cells were grown as described previously until ~70% confluence (to allow the observation of single cell membranes) and Chol removal induced by incubation overnight with 20 μg/ml apoA-I in serum-free medium, or by 10 mM MβCD for 30 min. Next, cells were washed with PBS and incubated for 15 min at 37°C with Laurdan to a final concentration 1 μM in Dulbecco modified Eagle medium (DMEM) with 2.5% FBS. Next, cells were washed and kept in DMEM at the same temperature during the observation time in a thermostatized microscope stage.

Other Analytical Methods

Protein was quantified by the method of Lowry et al. (1951). Transmission electron micrograph was acquired at the Centro de Microscopía Electrónica, Facultad de Veterinaria, UNLP, Buenos Aires, Argentina. Western blot testing for the detection of apoA-I and caveolin-1 was performed by traditional techniques as described above. To better determine the significance of intracellular levels of caveolin, four lines of each control and SCD cells were loaded into a gel and probed with against caveolin, after stripping and reprobing against β-actin as a housekeeping marker. Chol efflux toward MβCD or apoA-I was measured with the Amplex Red Commercial kit (Invitrogen). Unless otherwise stated, results are mean ± standard error of three independent measurements. Statistically significant differences between experimental conditions were evaluated by analysis of variance followed by Bonferroni's comparison test ($^*P < 0.05$ compared to control).

Results

Cell Line Construction

SCD catalyzes the conversion of stearoyl-CoA to oleoyl-CoA, and thereby it regulates the ratio of monounsaturated

to saturated fatty acids in cell membrane phospholipids (Enoch et al. 1976). The efficiency of SCD transfection and overexpression was confirmed by different methods. Northern blot testing showed high levels of ARNm as compared with almost undetectable amounts in the control cells (Fig. 1a); the same was observed when analyzing, by Western blot testing, protein expression levels (Fig. 1b). In this case, an upper faint band was observed with the same intensity for both types of cells, which was assumed to be the endogenous hamster SCD. Moreover, as expected (Sun et al. 2003), ABCA1 protein basal level was not significantly modified in SCD cells with respect to control (Fig. 1c).

PM Isolation and Composition

PM was isolated and lipid composition characterized. Figure 1d shows a typical elution profile of the cell fractionation obtained by ultracentrifugation. Selected fractions were pooled and further characterized. As the electron microscopy image shows (Fig. 1e), sample rearranged as close empty vesicles (as typically occurs with membrane preparations), and it was free of mitochondria. PM was confirmed by the presence of the standard enzyme marker Na–K ATPase, and it showed no contamination with endoplasmic reticulum (undetectable arylesterase activity). Figure 2 shows the comparative lipid composition of the isolated PM in SCD versus control cells. As expected, a significant increase in the 16:1/16:0 and 18:1/18:0 ratios confirmed the enzyme activity (Fig. 2a). In good agreement with Sun et al. (2003), there was an approximately 100% increase in SCD cells of both ratios as compared with control cells. Next, we analyzed the relative composition of the major neutral lipids. In an attempt to facilitate the comparative studies, we expressed the lipids as the mass ratio of glycerophospholipids (GPL) to SM, and GPL to FC. Figure 2b shows that SCD cells have a more than 50% higher GPL/SM ratio; instead, the GPL/FC ratio decreased by approximately 20%. The values in control cells were in good agreement with previous data by Cezanne et al. (1992).

Membrane Organization of Cells In Vivo

Our group (Sanchez et al. 2002, 2007a; Tricerri et al. 2005) and others (Gaus et al. 2003; Heiner et al. 2008; Montes et al. 2007; Smith et al. 2001) have previously used Laurdan GP imagining and two-photon excitation fluorescence

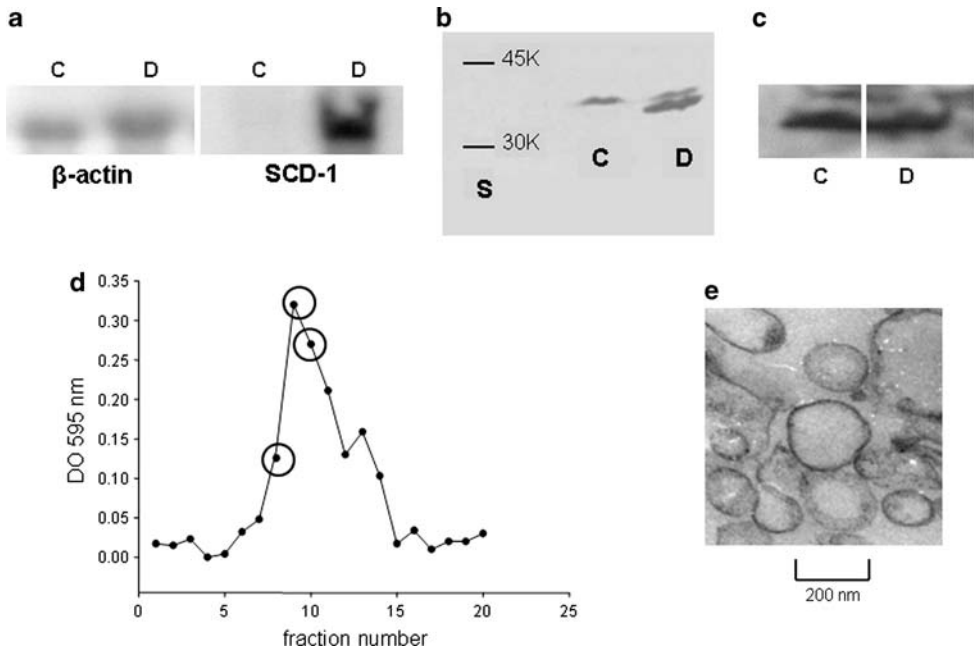

Fig. 1 SCD cell line characterization. **a** Overexpression of SCD determined by Northern blot test. Twenty micrograms of total RNA were loaded in each well, and SCD overexpression (D) with respect to control (C) was determined by comparison with β-actin, as described in Methods. **b** Protein levels of SCD detected by Western blot. One hundred fifty micrograms of total protein of the membrane pellet was resuspended in sample buffer containing SDS and β-mercaptoethanol, boiled, and resolved in a homogeneous 12% gel with 1% SDS. Lane S corresponds to molecular weight markers. **c** ABCA1 protein levels were detected in a similar manner. Samples without boiling treatment were separated in a 4–15% gradient gel containing SDS. **d** Typical elution profile obtained for membrane purification. Each 200 µl from the top of the Nicodenz–Ficoll gradient was tested for protein content (Bradford 1976). Fractions labeled with an empty circle were pooled and further analyzed to confirm the presence and purity of plasma membrane (PM). **e** Transmission electron micrograph of the isolated PM fraction (magnification, ×20,000)

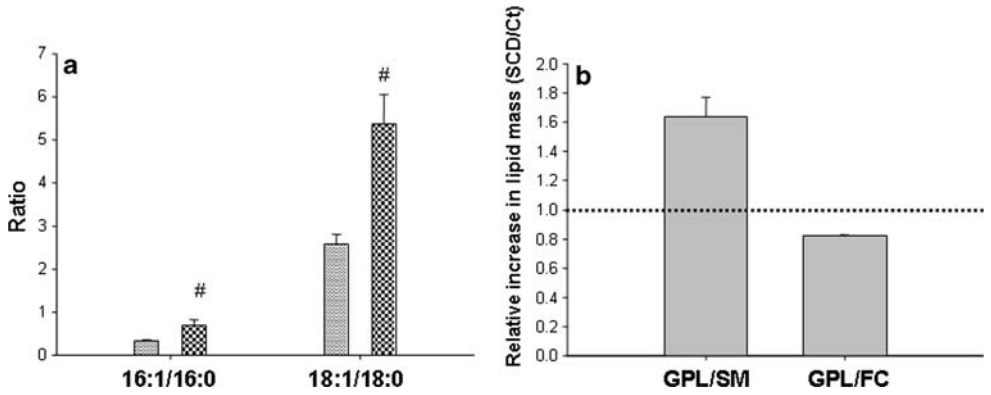

Fig. 2 Lipid composition of the SCD cells plasma membrane (PM) with respect to control cells. **a** Total lipids from the PM fraction were extracted, and fatty acid composition was determined by gas–liquid chromatography after transesterification with B_3F. *Bars* show 16:1/16:0 and 18:1/18:0 ratios of SCD cells (*checkered bars*) respect to control (*dashed bars*). # Significantly different as compared with control cells ($P < 0.05$). **b** Plasma total lipids were separated by TLC and composition quantified by scanning of different lipid areas after calcination. Shown are the relative ratios of glycerophospholipids (GPL) to sphingomyelin (SM) and to free cholesterol (FC) in SCD cells with respect to control (Ct) cells. *Dot line* shows ratio = 1 to better visualize the relative changes induced by the overexpression of SCD

microscopy to analyze membrane organization in artificial bilayers and in live cells. This technique offers the sole advantage of allowing the analysis of lateral organization without disruption of the observation system. Laurdan solubilizes equally into fluid or condensed membranes and is not associated with specific fatty acids or phospholipid head groups (Bagatolli et al. 2003). Thus, GP values reflect the overall membrane structure and not a specific lipid or protein composition (Harris et al. 2002).

Laurdan-labeled cells were imaged by setting the focal *z* plane in the middle of the cell, allowing the observation of PM (Fig. 3a). GP values can range from 1 to −1 according to Eq. 1, and an arbitrary color scale was used to visualize pixels with different GP values. One can use the SimFCS program to separate pixels associated with the PM (Fig. 3b) and select areas in which GP can be quantified without contamination of cellular debris present in the image (Fig. 3b, white circles). GP value was the average of the pixel distribution in the selected area (histogram in Fig. 3c). To avoid dispersion in the results due to laser alignment, cell confluence, and so on, each treatment with Chol acceptors (apoA-I or cyclodextrin) was compared to untreated cells measured in the same day under identical conditions.

This study reveals two interesting issues. First, even though some heterogeneities in the GP images could suggest presence of domains in the PM (Fig. 3a, b), we cannot clearly confirm the presence of "macrodomains" in the cells, as it is easily defined with artificial liposomes (Tricerri et al. 2005). Because Laurdan GP imaging can distinguish liquid-ordered (l_o) and liquid-disordered (l_d) macrodomains coexisting in the same bilayer (Sanchez et al. 2007a; So et al. 1995), we attributed this observation to the fact that domains are dynamic and move within the experimental time, and thus they are not usually detectable in live cells. Instead, Sun et al. (2003), using the same SCD construct and Triton X-100, visualized domain segregation with an increased amount of l_d in the PM of fixed cells. It is possible that the fixing and detergent treatment "freeze" the mobile existing membrane segregations. Second, despite the different lipid composition (Fig. 2), no significant changes in the membrane overall water content (i.e., fluidity) were observed between SCD cells and the control (Fig. 3d, e). Instead, when Chol was removed, GP changes depended on the cell type and the Chol acceptor. When apoA-I is used as Chol acceptor, the GP value decreased in both cases (Fig. 3d). Instead, if MβCD was used as acceptor, membrane GP increased for the control cells and decreased for SCD cells (Fig. 3e). To compare the efficiency of both acceptors, we measured Chol in the media at the end of the incubation times. ApoA-I-mediated Chol efflux was about half efficient than MβCD, which was also faster under the experimental conditions. In this case, higher amounts of Chol were solubilized from SCD cells (Fig. 4).

Effect of SCD Overexpression on Cell Functionality

We investigated the influence of SCD overexpression on mitochondrial reduction capacity. This test is widely used and has been inversely correlated with cytotoxicity (Melchert et al. 2001). Thus, higher optical density at 560 nm was related with an increased activity of metabolic cells, which induced the cleavage of the yellow tetrazolium salt MTT to purple formazan crystals. SCD cells showed ~17% higher mitochondrial activity (Fig. 5a) than control cells. Moreover, the incubation with apoA-I induced a higher MTT reduction activity in both types of cells. In

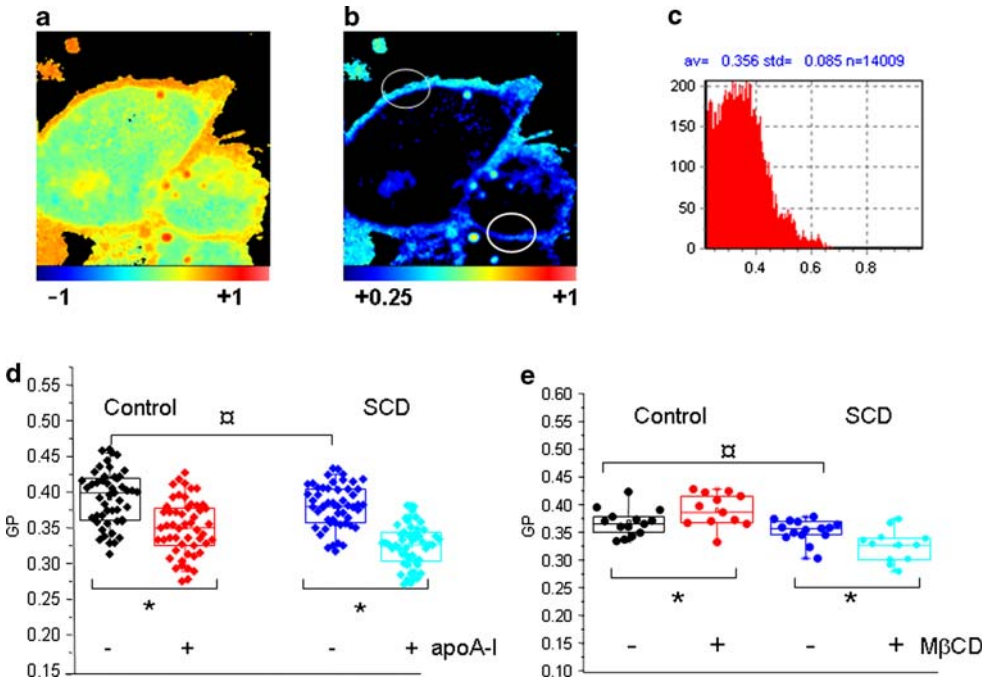

Fig. 3 Laurdan GP two-photon fluorescence microscopy of CHO cells. **a** Cells were grown as described previously and stained with Laurdan for 15 min. Laurdan GP images were taken as described, focusing at the middle plane of the cell. **b** As (**a**), but with a modification in the color scale to eliminate the interference of pixels with lower GP values (from the Laurdan solubilized into the cytoplasm; see scale). *Empty white circles* indicate the selected areas for GP analysis. Each histogram of GP values of these areas (represented in (**c**)) is used to calculate the experimental data shown in (**d**) and (**e**). **e** Experimental values of GP at the plasma membrane in unperturbed control (*black*) and SCD cells (*blue*). Box charts show minimum, 25th percentile, median, and 75th percentile values. GP was also measured in the same way after overnight incubation of control (*red*) and SCD cells (*cyan*) with 20 μg/ml apoA-I. No difference was detected among samples without addition of apoA-I (*currency sign*, $P < 0.05$). Instead, GP decreased significantly for both types of cells after the addition of apoA-I (*asterisk*, $P < 0.05$). **e** Cells (control and overexpressing SCD) were incubated in the absence or presence of 10 mM MβCD for 30 min. Experimental data are analyzed as in (**d**). As in (**d**), statistical nondifference is shown with *currency sign*, while *asterisk* represents a significant increase or decrease of membrane GP after treatment with MβCD of control or SCD cells, respectively ($P < 0.05$)

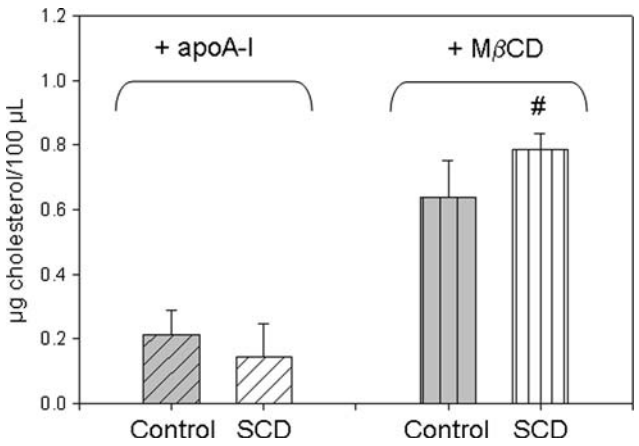

Fig. 4 Cholesterol (Chol) removal to different acceptors. Cells were in a 96-well plate and incubated as described above overnight in the presence of 20 μg/ml apoA-I (*diagonally lined bars*), or by 30 min with 10 mM βCD (*vertically lined bars*). Cholesterol in the media at the end of the treatments was analyzed as described in "Methods". * Statistical increase of Chol removal by SCD cells (*white bars*) with respect to control cells (*gray bars*) ($P < 0.05$)

addition, we measured the release of LDH, which was correlated with cytotoxicity (Peter et al. 2008). Control cells showed a higher release of LDH to the medium, indicating that SCD overexpression induces a beneficial effect on cell viability (Fig. 5b).

Intracellular Chol Esterification and Lipid Storage

Because intracellular Chol could be freed or stored as CEs, we measured radioactivity incorporated in CE after incubating cells with [^{3}H] Chol as described above, in the presence or absence of apoA-I. Our results showed a higher CE/FC ratio in SCD cells in comparison with control cells (not shown). It is well-known that in skin fibroblasts (Yamauchi et al. 2004) and in CHO cells (Gonzalez et al. 2008), apoA-I induced a decrease in the cellular Chol pool available to be esterified by acyl CoA:Chol acyltransferase. Thus, a decrease in the CE/FC ratio was expected when control cells were incubated with apoA-I, and the same was observed when apoA-I was incubated with SCD cells (data

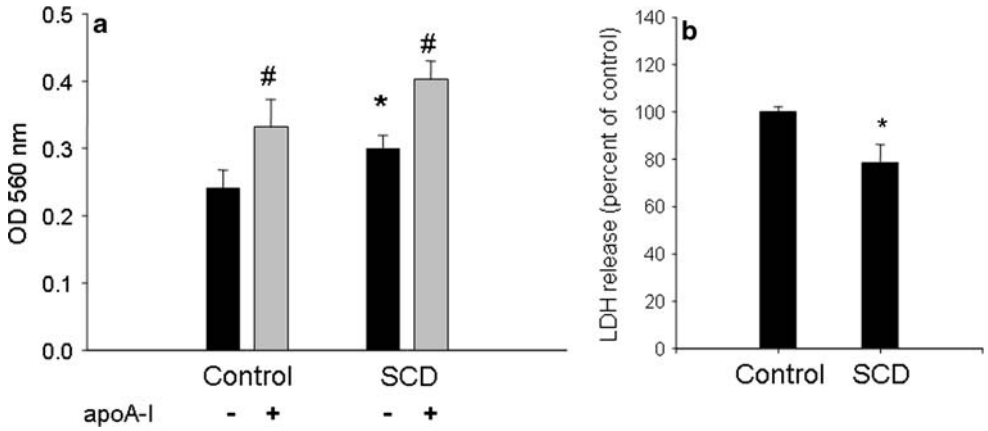

Fig. 5 Cellular viability. **a** Mitochondrial metabolism assay. Cells were grown in a 96-well microplate, and MTT reduction was evaluated with or without overnight incubation with 20 μg/ml apoA-I. The formation of formazan was quantified by absorbance at 560 nm (* $P < 0.05$ compared to control, untreated cultures; $^{\#}P < 0.05$ compared to the same type of cells incubated in the absence of apoA-I). Results are the means of five experimental points. **b** Lactate dehydrogenase (LDH) release into the medium. Cells were grown as explained in "Methods", and LDH in the medium was determined by kinetics of disappearance of nicotinamide adenine dinucleotide reduced form at 340 nm. Results are the means of triplicate samples (* $P < 0.05$ compared to control, untreated cultures)

not shown). We analyzed whether SCD overexpression could modify intracellular neutral lipid deposits. Figure 6 shows a significant increase of intracellular lipid droplets in these cells; it can be clearly observed as a larger amount of spots stained with Oil Red O reagent.

Caveolin Intracellular Levels and Exportation

Caveolin 1 is a 22-kDa protein. Even though most of the functions are currently unclear, it has been proposed to act as Chol sensors and to regulate lipid trafficking to and from specific membrane domains, such as caveolae rich in Chol and SM (Pol et al. 2004). It should therefore have intracellular and extracellular lipid transport-related functions. In addition, its expression has been associated with apoptosis in macrophages (Gargalovic and Dory 2003). To assess the probable relationship between membrane composition, lipid transport, and caveolin function, we measured caveolin-1 levels in cells and media in the presence and absence of apoA-I as a Chol acceptor. Figure 7a shows that intracellular levels of caveolin-1 are slightly but significantly decreased in SCD cells compared with control cells; apoA-I has no significant effect on the levels of this protein (data not shown). To characterize caveolin-1 exportation and study the influence that apoA-I could have in such event, we incubated cells as described above, and analyzed the extracellular medium by native gradient PAGE, with or without incubation with apoA-I for 12 h. Interestingly, caveolin-1 was significantly more exported in SCD-overexpressing cells, associated with products with molecular weights of approximately 80 and 150 kDa (Fig. 7b, i). Incubation with apoA-I did not induce a strong effect on such levels. In addition, to analyze the interaction of apoA-I with caveolin, we performed a gel under the same conditions but revealed it with a polyclonal anti-apoA-I antibody; as Fig. 7b, ii, shows, most of the apoA-I remains as small lipid-poor particles, and to a lesser extent as big complexes, probably associated with different amounts of solubilized lipids. Nevertheless, it is clear that no apoA-I was associated with the 80- or 150-kDa complexes comigrating with caveolin.

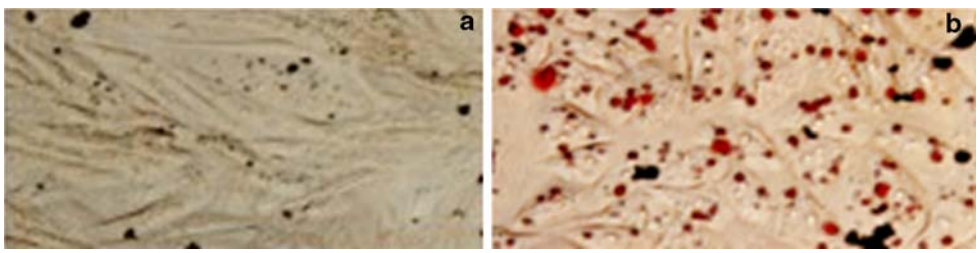

Fig. 6 Observation of intracellular lipid droplets. Cells were fixed and stained with Oil Red O as described in "Methods". Observation was made in an Olympus BX51 microscope. Intracellular red spots correspond to lipid accumulations. **a** Control cells and **b** SCD cells

Discussion

Mammalian cells are required to keep a dynamic arrangement of lipids and proteins as a basal mechanism to organize their structure and viability. Such events are strictly regulated by the membrane organization, which determines the intensity of multiple signaling cascades (Simons and Toomre 2000). Our results strongly support the hypothesis that PM composition is essential to avoid cytotoxic pools of Chol, thus helping cell viability. Many mechanisms could be involved in such events, and we will consider some of them here.

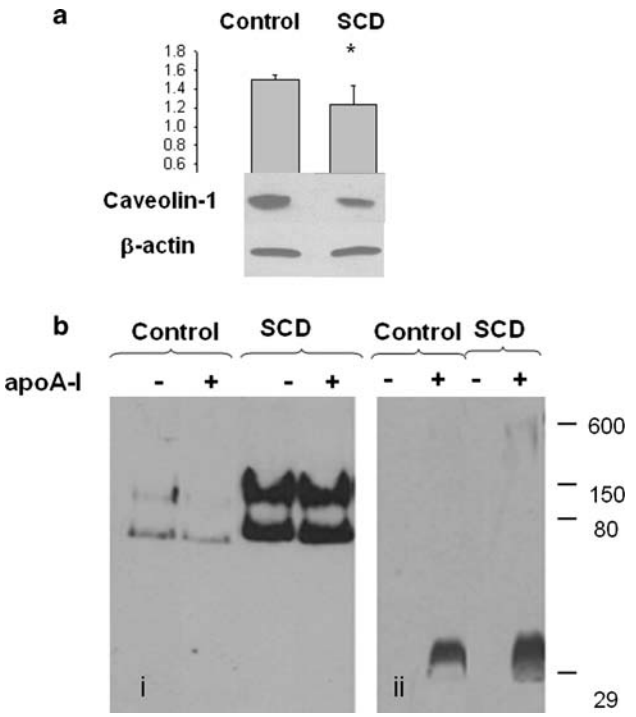

Fig. 7 Intracellular and exportation levels of caveolin-1. **a** Control and SCD cells were grown and incubated as previously described. Culture cells were scraped, lysed, and homogenized. The same amount of protein from the different treatments was loaded on a 12% PAGE with 1% SDS, Western blot developed against α-caveolin, and, after stripping, developed against β-actin. Bands of four different samples of control or SCD cells were scanned, and the relative intensity of each band was quantified by Image Quant software. The caveolin/actin ratio is averaged and is shown at the top (* $P < 0.05$ compared to control, untreated cultures). **b** Control and SCD cells were grown and incubated with apoA-I as previously described. After 12 h incubation with DMEM or apoA-I, media were collected, centrifuged for 15 min at 5,000*g*, and concentrated; the same amount of total protein of the different treatments was loaded on a native 4–25% polyacrylamide gradient electrophoresis gel (**b**, i) and revealed by polyclonal caveolin-1 antibody. (**b**, ii) An equivalent gel was loaded and run under exactly the same conditions, but revealed against polyclonal α-apoA-I. *Numbers* on the right correspond to molecular weight standards

Membrane Composition and Fluidity

As mentioned above, in spite of the different lipid composition, PM of SCD cell keeps the average water content (i.e., fluidity) than control cells. We considered this finding particularly interesting because it strongly suggests that SCD overexpression triggered compensating chemical changes to prevent alteration of the PM properties. This compensation could be explained by relative changes in Chol and SM (Fig. 2).

It was recently shown that a decrease in membrane fluidity favors Chol efflux (Nandi et al. 2009). As a result of the well-preserved water content that we observed for membranes of unperturbed cells (Fig. 3), we conclude that membrane fluidity is important to keep cell functionality but is probably not mediating Chol efflux.

Domains Organization and Cell Interaction with Different Chol Acceptors

Our results show that GP decreases when Chol is removed by apoA-I from both types of cells (Fig. 3d); instead, a significant increase of the GP at the PM of control cells and a decrease of the GP of SCD cell membranes (Fig. 3e) were observed when the Chol acceptor was MβCD. On the basis of our previous data that used model systems (Sanchez et al. 2007a), we suggest that Chol is solubilized from highly ordered domains from control cells, and from disordered domains from SCD cells. Nevertheless, as a result of the complexity of the membrane organization and the dynamics of lipid rearrangement, other possibilities cannot be discarded, although they are not discussed here. Clearly, the treatment with the two Chol acceptors (MβCD and apoA-I) reveals two issues: first, the control and SCD cell PMs are different but the cells in vivo compensate for this difference to keep their viability; and second, Chol efflux mediated by apoA-I and MβCD induces a different membrane lipid reorganization.

It was observed that SCD cells show a lower efficiency for Chol removal mediated by apoA-I. We have observed that this behavior is also valid when cells are loaded with external Chol (data not shown). This decreased efficiency for Chol efflux cannot be explained by a special membrane composition that binds Chol with high affinity; the lipid composition found in SCD cells, a significantly lower amount of SM, and an increase in unsaturated fatty acids should result instead in a higher tendency of Chol to "escape" from the membrane (Lange and Steck 2008; Simons and Vaz 2004) and hence to be exported. The fact that Chol removal by apoA-I increases mitochondrial activity preferentially from SCD cells suggests that the relative decrease of SM with respect to GPL induces domain organization with Chol solubilized into pools more

available to acceptors as apoA-I and then more favorable to be exported. Along this line of thought, it has been postulated that apoA-I removes a cytotoxic pool of Chol that is at the PM (Kellner-Weibel et al. 1999). Our data suggest that this pool could be selectively solubilized, especially from SCD, showing higher mitochondrial activity and less LDH release (Fig. 5).

Intracellular Trafficking

Closely related to the concepts mentioned above, intracellular mobilization of Chol is strongly dependent on membrane organization. It has been shown that the highest concentration of caveolin is found in the PM in caveolae that are rich in Chol and sphingolipids (Williams and Lisanti 2004). In addition to the membrane-bound state, this protein also has a soluble cytoplasmic form, as well as a secreted form, both of them embedded in lipoprotein-like particles (Liu et al. 1999, 2002). Our results showed that SCD cells presented lesser amounts of caveolin, probably as a result of a higher secretion. This effect could be explained to the lower relative amounts of SM respect to GPL at the PM, which destabilize caveolae and favor its exportation to the media (Fig. 7).

In addition, it is interesting that even though SCD cells show lower efficiency to export Chol (Sun et al. 2003), they are less susceptible to Chol cytotoxicity (Fig. 5). Our results support the fact that the lowest Chol efflux is associated with a higher cellular CE/FC ratio, and with a clear increment of intracellular lipid depots (Fig. 6). The decreased levels in caveolin could, as Frank et al. (2006) suggested, induce the increase observed in CE/FC ratio.

The characteristic of the exported caveolin is not well-known. Some cells secrete caveolin in high-density lipoproteins containing apoA-I, raising the possibility that caveolin-rich lipid particles in the cytoplasm are involved in the assembly of secreted lipoproteins and regulation of lipid export (Liu et al. 2002). These authors did not detect such type of vesicles in CHO cells, and our results showed that only a small amount of caveolin is secreted from control cells, either in the absence (Fig. 7b, i) or presence of apoA-I (Fig. 7b, ii). Instead, a significant amount of this protein showing a molecular weight of approximately 80 and 150 kDa is exported from SCD cells (Fig. 7 b, i, lines 3 and 4). It does not comigrate with apoA-I (Fig. 7b, ii), and it is associated with fractions of density higher than 1.21 g/ml (data not shown). Thus, these exportation products do not seem to be assembled as high-density lipoproteins but as caveolin oligomers disassembled from the PM as a result of the poor platform offered by lipids in SCD cells (low SM and high unsaturated phospholipids).

In conclusion, our results show that membrane composition and organization coordinate cellular pathways involved in Chol efflux and cell viability by different mechanisms. Although the entire membrane fluidity is preserved, disruption of SM-rich domains induces the solubilization of Chol into pools accessible to apoA-I and favors caveolin turnover which, in turn, builds up intracellular storages of nontoxic CEs. This signaling event might be complex, and some other proteins (such as SCP-2) are likely to participate in Chol transport and efflux. Further research will be focused in this field.

Acknowledgments The work presented here was supported by the Agencia Nacional de Promoción Científica y Tecnológica, Argentina, grants 14443 to OJR and 26228 to HAG, Consejo de Investigaciones Científicas y Técnicas (PIP 112-200801-00953 to HAG), and the Australian Fluorescence Foundation R108 and International Cooperation (CONICET) to MAT. We thank L. Hernandez for her expertise and technical support with apoA-I purification and figure preparation. OJR, HAG, MCG, and MAT are members of the Carrera del Investigador Científico (CONICET), Argentina. SS acknowledges the National Institutes of Health (grant PHS 5 P41 RR-03155, US).

References

Bagatolli LA, Sanchez SA, Hazlett T, Gratton E (2003) Giant vesicles, Laurdan, and two-photon fluorescence microscopy: evidence of lipid lateral separation in bilayers. Methods Enzymol 360:481–500

Bligh EG, Dyer WJ (1959) A rapid method of total lipid extraction and purification. Can J Biochem Physiol 37:911–917

Bradford MM (1976) A rapid and sensitive method for the quantitation of microgram quantities of protein utilizing the principle of protein-dye binding. Anal Biochem 72:248–254

Cezanne L, Navarro L, Tocanne JF (1992) Isolation of the plasma membrane and organelles from Chinese hamster ovary cells. Biochim Biophys Acta 1112:205–214

De Felice FG, Houzel JC, Garcia-Abreu J, Louzada PR Jr, Afonso RC, Meirelles MN, Lent R, Neto VM, Ferreira ST (2001) Inhibition of Alzheimer's disease beta-amyloid aggregation, neurotoxicity, and in vivo deposition by nitrophenols: implications for Alzheimer's therapy. FASEB J 15:1297–1299

Enoch HG, Catala A, Strittmatter P (1976) Mechanism of rat liver microsomal stearyl-CoA desaturase. Studies of the substrate specificity, enzyme–substrate interactions, and the function of lipid. J Biol Chem 251:5095–5103

Fielding PE, Nagao K, Hakamata H, Chimini G, Fielding CJ (2000) A two-step mechanism for free cholesterol and phospholipid efflux from human vascular cells to apolipoprotein A-1. Biochemistry 39:14113–14120

Folch J, Lees M, Stanley GHS (1957) A simple method for the isolation and purification of total lipides from animal tissues. J Biol Chem 226:497–509

Frank PG, Cheung MW, Pavlides S, Llaverias G, Park DS, Lisanti MP (2006) Caveolin-1 and regulation of cellular cholesterol homeostasis. Am J Physiol Heart Circ Physiol 291:H677–H686

Gargalovic P, Dory L (2003) Cellular apoptosis is associated with increased caveolin-1 expression in macrophages. J Lipid Res 44:1622–1632

Gaus K, Gratton E, Kable EP, Jones AS, Gelissen I, Kritharides L, Jessup W (2003) Visualizing lipid structure and raft domains in living cells with two-photon microscopy. Proc Natl Acad Sci USA 100:15554–15559

Gonzalez MC, Toledo JD, Tricerri MA, Garda HA (2008) The central type Y amphipathic alpha-helices of apolipoprotein AI are involved in the mobilization of intracellular cholesterol depots. Arch Biochem Biophys 473:34–41

Harris FM, Best KB, Bell JD (2002) Use of laurdan fluorescence intensity and polarization to distinguish between changes in membrane fluidity and phospholipid order. Biochim Biophys Acta 1565:123–128

Heiner AL, Gibbons E, Fairbourn JL, Gonzalez LJ, McLemore CO, Brueseke TJ, Judd AM, Bell JD (2008) Effects of cholesterol on physical properties of human erythrocyte membranes: impact on susceptibility to hydrolysis by secretory phospholipase A2. Biophys J 94:3084–3093

Jacobson K, Mouritsen OG, Anderson RG (2007) Lipid rafts: at a crossroad between cell biology and physics. Nat Cell Biol 9:7–14

Kellner-Weibel G, Geng YJ, Rothblat GH (1999) Cytotoxic cholesterol is generated by the hydrolysis of cytoplasmic cholesteryl ester and transported to the plasma membrane. Atherosclerosis 146:309–319

Lange Y, Steck TL (2008) Cholesterol homeostasis and the escape tendency (activity) of plasma membrane cholesterol. Prog Lipid Res 47:319–332

Liu P, Li WP, Machleidt T, Anderson RG (1999) Identification of caveolin-1 in lipoprotein particles secreted by exocrine cells. Nat Cell Biol 1:369–375

Liu P, Rudick M, Anderson RG (2002) Multiple functions of caveolin-1. J Biol Chem 277:41295–41298

Lowry OH, Rosebrough NJ, Farr AL, Randall RJ (1951) Protein measurement with the Folin phenol reagent. J Biol Chem 193:265–275

Mander EL, Dean RT, Stanley KK, Jessup W (1994) Apolipoprotein B of oxidized LDL accumulates in the lysosomes of macrophages. Biochim Biophys Acta 1212:80–92

Melchert RB, Liu H, Granberry MC, Kennedy RH (2001) Lovastatin inhibits phenylephrine-induced ERK activation and growth of cardiac. Cardiovasc Toxicol 1:237–252

Mendez AJ, Lin G, Wade DP, Lawn RM, Oram JF (2001) Membrane lipid domains distinct from cholesterol/sphingomyelin-rich rafts are involved in the ABCA1-mediated lipid secretory pathway. J Biol Chem 276:3158–3166

Montes LR, Alonso A, Goni FM, Bagatolli LA (2007) Giant unilamellar vesicles electroformed from native membranes and organic lipid mixtures under physiological conditions. Biophys J 93:3548–3554

Nandi S, Ma L, Denis M, Karwatsky J, Li Z, Jiang XC, Zha X (2009) ABCA1-mediated cholesterol efflux generates microparticles in addition to HDL through processes governed by membrane rigidity. J Lipid Res 50:456–466

Oram JF (2002) ATP-binding cassette transporter A1 and cholesterol trafficking. Curr Opin Lipidol 13:373–381

Oram JF, Heinecke JW (2005) ATP-binding cassette transporter A1: a cell cholesterol exporter that protects against cardiovascular disease. Physiol Rev 85:1343–1372

Parasassi T, Gratton E (1995) Membrane lipid domains and dynamics as detected by Laurdan fluorescence. J Fluoresc 8:365–373

Parasassi T, Gratton E, Yu WM, Wilson P, Levi M (1997) Two-photon fluorescence microscopy of laurdan generalized polarization domains in model and natural membranes. Biophys J 72:2413–2429

Peter A, Weigert C, Staiger H, Rittig K, Cegan A, Lutz P, Machicao F, Haring HU, Schleicher E (2008) Induction of stearoyl-CoA desaturase protects human arterial endothelial cells against lipotoxicity. Am J Physiol Endocrinol Metab 295:E339–E349

Pol A, Martin S, Fernandez MA, Ferguson C, Carozzi A, Luetterforst R, Enrich C, Parton RG (2004) Dynamic and regulated association of caveolin with lipid bodies: modulation of lipid body motility and function by a dominant negative mutant. Mol Biol Cell 15:99–110

Prinz WA (2007) Non-vesicular sterol transport in cells. Prog Lipid Res 46:297–314

Sambrook J, Fritsch EF, Maniatis T (eds) (1989) Molecular cloning: a laboratory manual. Cold Spring Harbor Press, Cold Spring Harbor, New York, pp 938–957

Sanchez SA, Bagatolli LA, Gratton E, Hazlett TL (2002) A two-photon view of an enzyme at work: Crotalus atrox venom PLA2 interaction with single-lipid and mixed-lipid giant unilamellar vesicles. Biophys J 82:2232–2243

Sanchez SA, Tricerri MA, Gratton E (2007a) Interaction of high density lipoprotein particles with membranes containing cholesterol. J Lipid Res 48:1689–1700

Sanchez SA, Tricerri MA, Gunther G, Gratton E (2007b) Laurdan generalized polarization: from cuvette to microscope. In: Méndez-Vilas A, Díaz J (eds) Modern research and educational topics in microscopy: applications in physical/chemical sciences. Formatex Research Center, Badajoz, Spain, pp 1007–1014

Schroeder F, Gallegos AM, Atshaves BP, Storey SM, McIntosh AL, Petrescu AD, Huang H, Starodub O, Chao H, Yang H, Frolov A, Kier AB (2001) Recent advances in membrane microdomains: rafts, caveolae, and intracellular cholesterol trafficking. Exp Biol Med (Maywood) 226:873–890

Schroeder F, Atshaves BP, McIntosh AL, Gallegos AM, Storey SM, Parr RD, Jefferson JR, Ball JM, Kier AB (2007) Sterol carrier protein-2: new roles in regulating lipid rafts and signaling. Biochim Biophys Acta 1771:700–718

Simons K, Toomre D (2000) Lipid rafts and signal transduction. Nat Rev Mol Cell Biol 1:31–39

Simons K, Vaz WL (2004) Model systems, lipid rafts, and cell membranes. Annu Rev Biophys Biomol Struct 33:269–295

Smith SK, Farnbach AR, Harris FM, Hawes AC, Jackson LR, Judd AM, Vest RS, Sanchez S, Bell JD (2001) Mechanisms by which intracellular calcium induces susceptibility to secretory phospholipase A2 in human erythrocytes. J Biol Chem 276:22732–22741

Smith JD, Le Goff W, Settle M, Brubaker G, Waelde C, Horwitz A, Oda MN (2004) ABCA1 mediates concurrent cholesterol and phospholipid efflux to apolipoprotein A-I. J Lipid Res 45:635–644

So PTC, French T, Yu WM, Berland KM, Dong CY, Gratton E (1995) Time resolved fluorescence microscopy using two photon excitation. Bioimaging 3:49–63

Storey SM, Gallegos AM, Atshaves BP, McIntosh AL, Martin GG, Parr RD, Landrock KK, Kier AB, Ball JM, Schroeder F (2007) Selective cholesterol dynamics between lipoproteins and caveolae/lipid rafts. Biochemistry 46:13891–13906

Sun Y, Hao M, Luo Y, Liang CP, Silver DL, Cheng C, Maxfield FR, Tall AR (2003) Stearoyl-CoA desaturase inhibits ATP-binding cassette transporter A1-mediated cholesterol efflux and modulates membrane domain structure. J Biol Chem 278:5813–5820

Sviridov D, Fidge N, Beaumier-Gallon G, Fielding C (2001) Apolipoprotein A-I stimulates the transport of intracellular cholesterol to cell-surface cholesterol-rich domains (caveolae). Biochem J 358:79–86

Tricerri A, Corsico B, Toledo JD, Garda HA, Brenner RR (1998) Conformation of apolipoprotein AI in reconstituted lipoprotein particles and particle-membrane interaction: effect of cholesterol. Biochim Biophys Acta 1391:67–78

Tricerri MA, Toledo JD, Sanchez SA, Hazlett TL, Gratton E, Jonas A, Garda HA (2005) Visualization and analysis of apolipoprotein A-I interaction with binary phospholipid bilayers. J Lipid Res 46:669–678

Weber G, Farris FJ (1979) Synthesis and spectral properties of a hydrophobic fluorescent probe: 6-propionyl-2-(dimethylamino)naphthalene. Biochemistry 18:3075–3078

Williams TM, Lisanti MP (2004) The caveolin proteins. Genome Biol 5:214

Yamauchi Y, Chang CC, Hayashi M, Abe-Dohmae S, Reid PC, Chang TY, Yokoyama S (2004) Intracellular cholesterol mobilization involved in the ABCA1/apolipoprotein-mediated assembly of high density lipoprotein in fibroblasts. J Lipid Res 45:1943–1951

Yancey PG, Bortnick AE, Kellner-Weibel G, de la Llera-Moya M, Phillips MC, Rothblat GH (2003) Importance of different pathways of cellular cholesterol efflux. Arterioscler Thromb Vasc Biol 23:712–719